Frontal Photopolymerization with Convection

Michaël Belk,*,† Konstantin G. Kostarev,‡ Vitaly Volpert,† and Tamara M. Yudina‡

Laboratoire de Mathématiques Appliquees, UMR 5585 CNRS, Université Lyon 1, 69622 Villeurbanne, France, and Institute of Continuous Media Mechanics, Ural Branch of RAS, 1, Ac. Koralev Str., Perm, 614013, Russia

Received: December 11, 2002; In Final Form: May 23, 2003

In this paper, the development of frontal polymerization under conditions of free convective motion of a reactive mixture is studied experimentally and numerically. The convection is caused by the reaction exothermicity and by the density change, because the polymer is more dense than the monomer. The propagation of polymerization fronts with convection is studied for the photoinitiated polymerization of an aqueous solution of acrylamide. Comparison of terrestrial and space experiments with the results of numerical simulation shows that convection can lead to the formation of inhomogeneities in the polymer product; it can change the speed of propagation of the reaction front and even change the reaction from frontal to volumetric.

1. Introduction

At the present time, frontal polymerization of liquid monomers is one of the most promising trends in the synthesis of polymers. Because of the fact that the reaction zone occupies a rather small portion of the reactor, the frontal polymerization proceeds as a continuous, easily controlled process. It can be realized if the reaction is sufficiently exothermic and highly activated. It was first suggested for the polymerization of methyl metacrylate[1] and later was used for various polymerizing systems (see the work of Davtyan et al.[2] and Pojman and coworkers,[3,4] and the references therein). Among the numerous phenomena that can accompany the propagation of polymerization fronts, natural convection can be particularly important. It can change the velocity of its propagation, the stability of the fronts, and its very existence.[5−10] It is known, for example, that convection can lead to extinction of the front or change the reaction from frontal to volumetric, where it occurs simultaneously in the entire reactor.

The contribution of convection to the development of frontal polymerization is mainly determined by the intensity of the monomer motion. From the viewpoint of the analysis of the experimental results, the most complicated process is polymerization under conditions of weak convection. In this case, the existence of the polymerization front can be established by traditional physical−chemical methods (sampling, thermocouple measurements, pH indicators); however, to determine the temperature and concentration distributions, we need more precise experimental techniques.

The application of optical methods allows us to determine the conversion distribution—that is, the relative polymer concentration—and the actual boundaries of the polymerization front. In this work, we study the influence of convection on the evolution of the frontal polymerization, both experimentally and numerically. The Fiseau interferometer method is used to visualize the conversion distribution of the mixture.[11] In our experiments, we study the photoinitiated polymerization of the reaction mixture that is prepared from a 15% aqueous solution of acrylamide, and a small amount of methylenebisacrylamide served as a cross-linking agent. The reaction was initiated by adding a combination of riboflavin and tetramethylenediamine to the mixture.[12] In the initial state, the reaction mixture was a transparent liquid with Newtonian properties; the viscosity and density values of the reaction mixture were similar to those of water. The product of the reaction was a cross-linked poly(acrylamide) gel (PAG) that exhibited elastic properties.

The experimental techniques and results are described in more detail in the following section. In Section 3, we present a mathematical model to describe the photopolymerization with convection and compare the experiments and the numerical simulations.

2. Experiments

2.1. Techniques. The experimental reactor was a horizontal rectangular cell (areal dimensions of 90 mm × 35 mm) with a height of 1−10 mm. The upper and lower boundaries were formed by glass plates, which, when exposed to a monochromatic light from above, represented a working cell of the interferometer. The reaction was initiated by the illumination of the short side wall. For the gel polymerization, we used a model CD1-7 lamp (Ministerstvo srednego mashinostroeniya) with the radiation intensity of 1200 lx. The luminous flux passed through the diaphragms to fit the cell dimensions. In addition to the diaphragms, a heat filter was placed between the lamp and the cell. The exposure time was 1 h.

The experiments were conducted under nonisothermal conditions at an average ambient temperature of 300 K. During the reaction, the temperature of the mixture in the cell was measured by centrally located copper−constantan thermocouples. The maximum temperature difference was determined to be no more than 2 K for polymerization in thin cuvettes (∼1 mm) and ∼10 K in cuvettes that were 10 mm thick. For the main group of experiments, thermal measurements were not performed, to avoid perturbation of the polymerization front.

For the experimental investigations, we used the Fiseau interferometer to visualize variations in the refraction index of the reaction mixture, which are caused by temperature and

* Author to whom correspondence should be addressed. E-mail: belk@maply.univ-lyon1.fr.
† Université Lyon 1.
‡ Institute of Continuous Media Mechanics.

10.1021/jp0276855 CCC: $25.00
Published on Web 08/22/2003

conversion gradients during polymerization. Because of the careful selection of the reaction mixture, the refraction index changes, mainly as a result of the monomer conversion. The contribution of temperature gradients to the formation of interference patterns is not essential, being 1%−2% of the total change in the refraction index in thin cuvettes and ∼5%−7% in cuvettes that were 10 mm thick. Therefore, the variation of the refraction index can be associated with the conversion distribution.

Verification of the proposed technique was based on the results of gelation in the case without convection.[12] In terrestrial conditions, the development of gel formation without free convection is possible, because of a drastic increase of monomer viscosity in the reaction zone and compatibility of the heat wave and polymerization front velocities. This situation causes the heat wave generated in the course of reaction to propagate in a highly viscous liquid, which makes it incapable of initiating the convective motion. Bearing in mind that the viscosity of the reacting monomer decreases as the temperature increases, we also prevented the initiation of convection in our experiments through the use of 1.2-mm-thick cuvettes that had a high cuvette-to-monomer mass ratio, which prohibited overheating of the mixture and provided intensive heat removal through the lower wall.

The convection-free experiments were used as test cases: if the interference bands remained the same, then the propagation of the reaction front was not accompanied by convection.

Before proceeding to the analysis of our experiments, we briefly outline the results of an analytical investigation of photoinitiated polymerization in the absence of mass transfer. Here, our primary interest is with the fact that the rate of monomer conversion is proportional to the square root of the light intensity. According to the Burger-Lambert-Beer law, the intensity of light passing through an absorbing medium decreases exponentially, which, at the very beginning of reaction, generates an initial distribution of conversion in a liquid monomer, approaching its maximum value at the illuminated surface. As soon as the monomer conversion is high enough to generate a three-dimensional polymeric net, a stratified gel formation is observed at the near-wall region. Later, the boundaries of the polymerized region (the front of polymerization) advance into the monomer with a velocity that is determined by the net coefficient of light absorption, which is the algebraic sum of the absorption coefficients of all the mixture components. It should be emphasized here that the essential light absorption is related only to the activation of photoinitiator molecules, whereas variation of the front position with time is described by the logarithmic law. Otherwise, this relationship is more complicated.

2.2. Results. In our experiments, the visualized distribution of the monomer conversion in the reaction zone in the absence of convection appeared as a system of collinear interference bands spreading with time from the illuminated wall of the reactor (see Figure 1). Comparison of the total number of interference bands in the front of gel formation with the results of measurement of the final monomer conversion behind the front showed that, for 1.2-mm cuvettes, a transition from one band to the other occurred when PAG conversion changed by ∼2%. Visualization shows that the development of reaction in the bulk of the monomer—in particular, formation of the conversion distribution—does not start immediately after switching on the initiating lamp but, instead, starts some time later. This time interval t_0 can be defined as the induction period of the reaction. The appearance of this interval is possibly attributed to the fact that the rate of the initiator transition to an active form and the rate of formation of polymer chains under the action of an activated initiator are different.

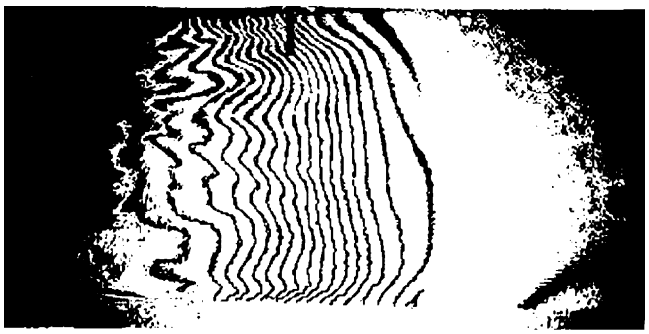

Figure 1. Interferogram of photoinitiated polymerization of PAG (left) in the absence of convection in a thin horizontal cuvette ($a = 1.2$ mm). View from above, $t = 38$ min.

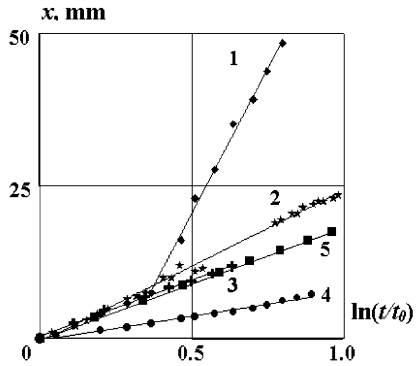

Figure 2. Propagation of the frontal reaction along the reactor under different gravity conditions: (1) reaction at weak convection (horizontal cuvette, $a = 10$ mm); the boundary of the reaction is defined by the position of gel film at the cuvette bottom (before the curve break), and the position of the "enriched" monomer evolved by convection (after the curve break); (2) gel front in the experiments on the "Mir" orbital station (1992) ($a = 10$ mm); (3) gel front in the absence of convection under laboratory conditions (horizontal cuvette, $a = 1.2$ mm); (4) gel front in the case of weak convection (horizontal cuvette, $a = 10$ mm); and (5) numerical simulation of the gel front in the absence of convection (horizontal cuvette, $a = 10$ mm).

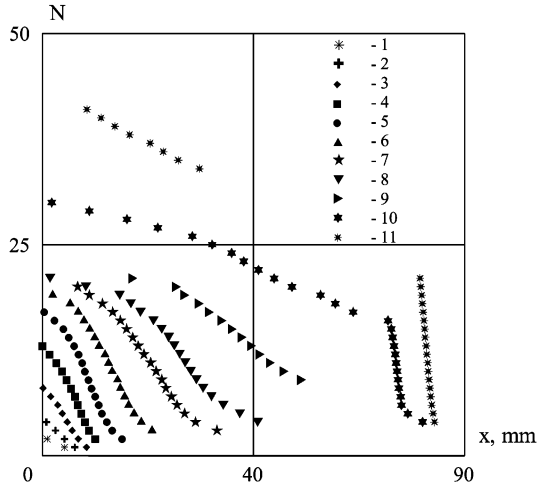

Figure 3. Distribution of the monomer conversion in the reactor (horizontal cuvette, $a = 1.2$ mm); x is the distance from the illuminated side of the reactor, N is the number of interference bands (each band corresponds to 0.25% conversion), and $t - t_0$ is the time of reaction ($t - t_0 =$ (1) 1 min; (2) 2.5 min; (3) 4.5 min; (4) 7.5 min; (5) 12.5 min; (6) 18.5 min; (7) 28 min; (8) 36 min; (9) 46 min; (10) 1 h, 30 min; and (11) 24 h).

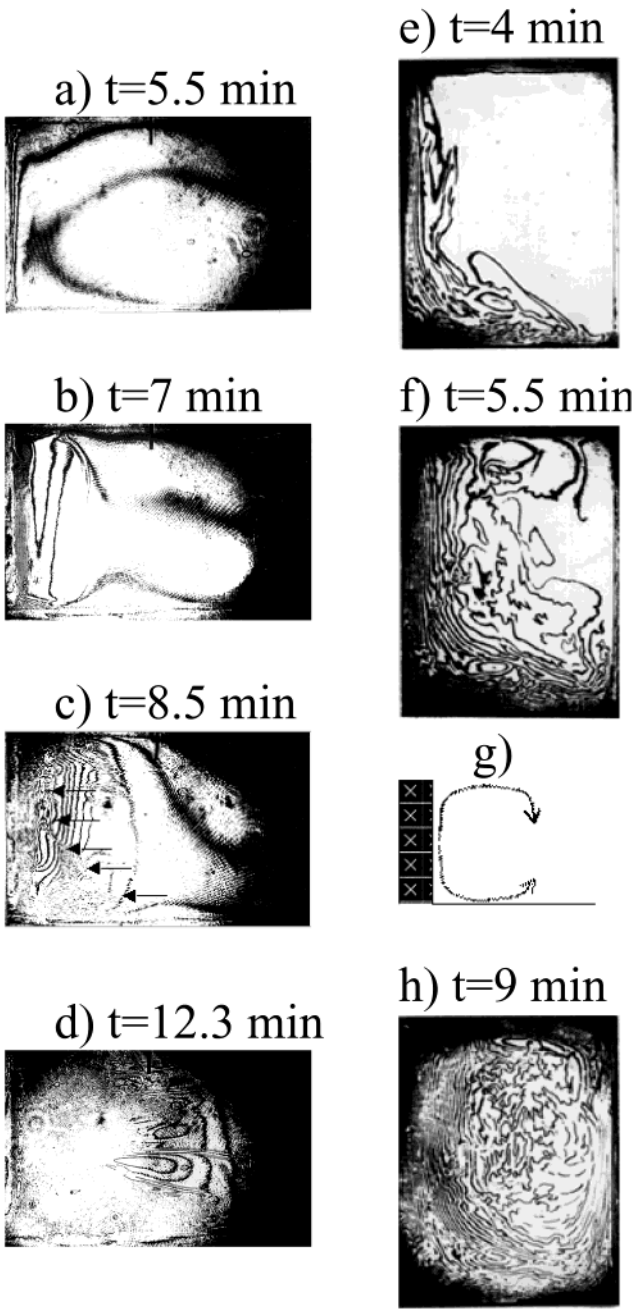

Figure 4. Interferograms of the photoinitiated gel formation in the case of weak convection ($a = 10$ mm). Panels a−d shows the horizontal cuvette, viewed from above. Each interference band corresponds to 0.25% conversion. Panels e, f, and h show the vertical cuvette, viewed from the side view. Panel g is a schematic representation of the monomer motion.

The use of the first interference band as the boundary of the reaction zone allows us to study the propagation of the polymerization front in a motionless monomer (see Figure 2, curve 3). Here, t is the reference time, which is taken to be the time that the initiating lamp is on, and x is the distance from the illuminated side of the reactor. As shown in the figure, the behavior of the curve is well described by the logarithmic law, which supports the statement that the light is absorbed only by the reaction initiator. Note that curve 2 in Figure 2 was obtained for the photopolymerization of PAG under conditions of orbital flight (the "Mir" station, 1992[13,14]).

Figure 3 shows the conversion distribution in the reactor for different moments of time. To simplify the comparison of the curves with the interferograms, the local degree of monomer conversion plotted on the ordinate is defined in terms of the number of interference bands N. Thus, curve 8 in Figure 3 describes the distribution of conversion for the interferogram shown in Figure 1.

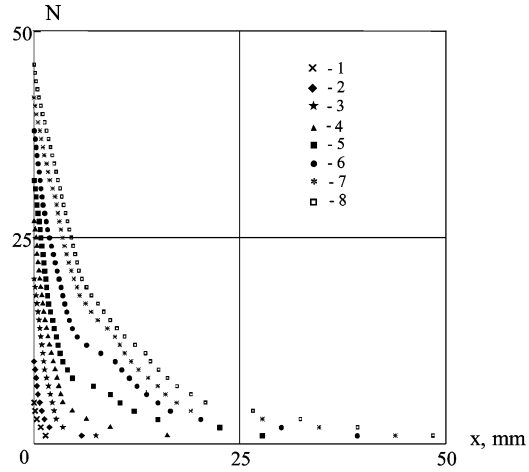

Figure 5. Distribution of monomer conversion in the reactor in the case of weak convection (horizontal cuvette, $a = 10$ mm); x is the distance from the illuminated side of the reactor, N is the number of interference bands (each band corresponds to 0.25% conversion) and $t - t_0$ is the time of reaction ($t - t_0 =$ (1) 1 min, (2) 1.5 min, (3) 2 min, (4) 5.5 min, (5) 6.5 min, (6) 7.5 min, (7) 8 min, and (8) 8.5 min).

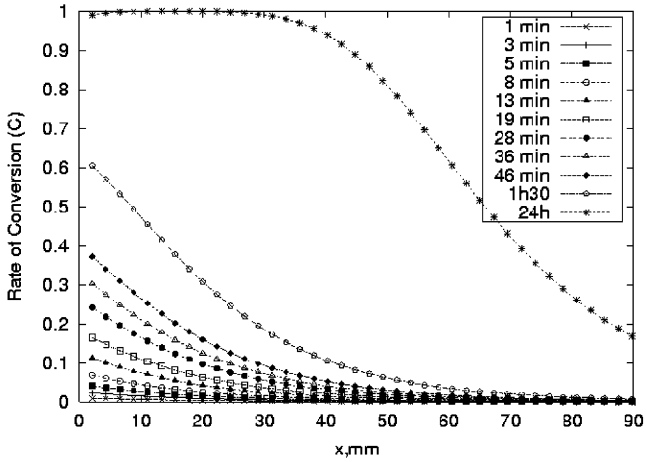

Figure 6. Distribution of the monomer conversion in the reactor in the absence of convection (numerical simulation).

The reaction behavior essentially changes with the appearance of convective motion in the monomer. To illustrate this effect, let us analyze the results of the experiment on photoinitiated gel formation in the case of a weak convection in a 10-mm-thick horizontal cuvette (interferograms in the left-hand side of Figure 4, which are views from above). In this case, the transition from one interferometric band to another equals a 0.25% change of the monomer conversion. The interferograms of the PAG polymerization in a vertical cuvette are shown in the right-hand side of Figure 4; in these interferograms, the reaction was initiated from the left-hand side and visualized sideways. Comparison of both interferogram series allows us to reconstruct a three-dimensional picture of the reaction development on the qualitative level.

Compared to gel formation in a quiescent medium, the conversion field structure becomes more complicated, although the isolines of the conversion initially remain parallel to the illuminated surface (see Figure 4a). The growth of the monomer mass involved in the reaction causes an enhanced heat flux along the reactor and diminishes the influence of adhesion, relative

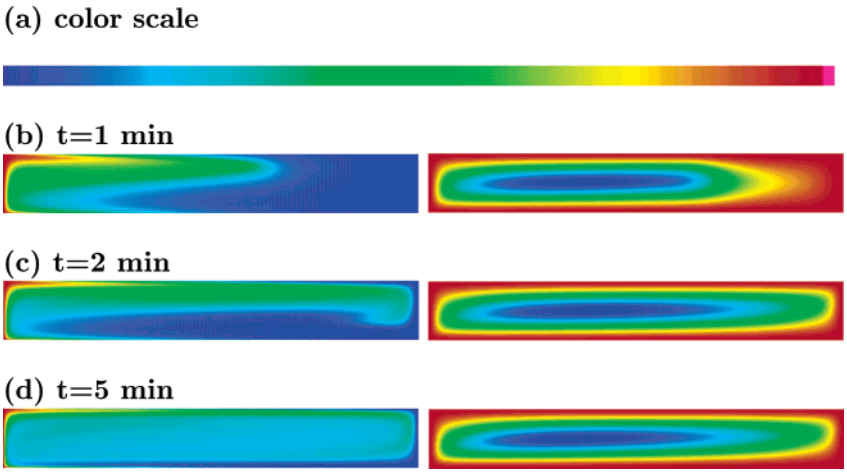

Figure 7. Monomer conversion (left) and stream lines (right) in the presence of convection (numerical simulation with $\beta_T \neq 0$, $\beta_C = 0$). Panel a shows the scale of colors. Conversion and stream function data are as follows: (b) $t = 1$ min; conversion: blue = 0.000218, red = 0.0102; stream function: blue = −0.0265, red = 0; (c) $t = 2$ min; conversion: blue = 0.000435, red = 0.0204; stream function: blue = −0.0242, red = 0; (d) $t = 5$ min; conversion: blue = 0.00109, red = 0.0502; stream function: blue = −0.0214, red = 0.

to the gravitational force. On one hand, these changes lead to instability of the polymerization front, which, in a gel, manifests itself as a downflow of a viscous (with high degree of conversion) reaction mixture from the monomer−polymer interface (see Figure 4e). The forming polymer, which sinks to the bottom, propagates at a higher velocity, compared to the true polymerization front. On the other hand, the front instability that disturbs the temperature and conversion distribution facilitates the development of convective motion in the monomer.

Convection, in its turn, causes the mixture with a lower conversion degree (compared to that of the sinking monomer) to leave the zone of the frontal reaction and move along the upper reactor boundary (see Figure 4b and f). This portion of the monomer, when moving, is also involved in polymerization, and its density gradually increases, in comparison with that of the original monomer. Finally, the upper layer of the polymerizing monomer loses its stability, falls down (this portion of the monomer is marked by the arrows in Figure 4c), and intermixes with the polymer spread over the bottom (see Figure 4g). The arising polymer wall generates a secondary polymerization front, forming several cells. These cells, which are filled with monomer, are left behind the secondary reaction front and can be seen for a long time on the following interferograms. Retention of the monomer between the two polymerization fronts is responsible for increasing the inhomogenity of the photoinitiated reaction. For a similar reason, the character of the convective motion becomes more complicated. The one-cell flow is replaced with a jet flow that pushes the partially reacted monomer forward. The latter is actively involved in polymerization, which changes its viscosity locally. As a result, the region of the reaction is subdivided into several longitudinal cells, in which polymerization proceeds at different rates (see Figure 4d). Clearly, the final structure of PAG formed under such conditions is essentially inhomogeneous (see Figure 4h).

The appearance of reacting monomer fluxes from the gel formation zone suggests that we should introduce two variables for an adequate description of polymerization evolution: (i) the boundary of the actual polymerization front that is associated with the formation of the uniform (continuous) polymer layer (see Figure 2, curve 4), and (ii) the boundary of the reaction propagation that is specified by the location of the polymerizing monomer spread along the bottom (the part of curve 1 up to the bending point in Figure 2) or washed out by the flow (the part of curve 1 after the bending point in the same figure).

Distributions of the PAG conversion formed during photopolymerization under conditions of convective flow are given in Figure 5, which shows the growth of the conversion gradients in the zone of gel formation and, simultaneously, the extension of the region, in which the polymerizing mixture has a low conversion, because of a monomer flow.

It follows from Figure 2 that, even in the case of a weak convection, the velocity of the reaction front increases (by a factor of ~7). Recent experiments[15] show that the opposite behavior can occur, because of an increase in convection intensity. The volume of the reaction mixture washed out of the near-front region grows, and, consequently, the average conversion degree of the monomer in the remainder of the reactor increases. Simultaneously, the velocity of the polymerization front decreases until the polymerization stops.

3. Numerical Simulations

3.1. Mathematical Model. In this section, we present the mathematical model that describes photopolymerization with convection. The system of equations consists of reaction−diffusion equations with convective terms, in addition to the Navier−Stokes equations under the Boussinesq approximation:

$$\frac{\partial T}{\partial t} + u\frac{\partial T}{\partial x} + v\frac{\partial T}{\partial y} - \kappa\Delta T = qk(T)\sqrt{s_1 \alpha JI}(1 - C) \quad (1)$$

$$\frac{\partial C}{\partial t} + u\frac{\partial C}{\partial x} + v\frac{\partial C}{\partial y} = k(T)\sqrt{s_1 \alpha JI}(1 - C) \quad (2)$$

$$\frac{\partial I}{\partial t} + u\frac{\partial I}{\partial x} + v\frac{\partial I}{\partial y} = -\alpha JI \quad (3)$$

$$\frac{\partial \vec{U}}{\partial t} + (\vec{U}\cdot\nabla)\vec{U} - \nu\Delta\vec{U} = -\frac{1}{\rho}\nabla p + [\beta_T(T - T_0) + \beta_C C]g\vec{\gamma} \quad (4)$$

$$\mathrm{div}\vec{U} = 0 \quad (5)$$

Here, T is the temperature of the mixture, C is the depth of conversion (that is, the dimensionless concentration of the product of the reaction ($0 \leq C \leq 1$)), I is the concentration of the initiator, q is the adiabatic heat release, s_1 and s_2 are scaling coefficients, α is the molar absorption coefficient, κ is the thermal diffusivity, and $k(T)$ is the temperature dependence of

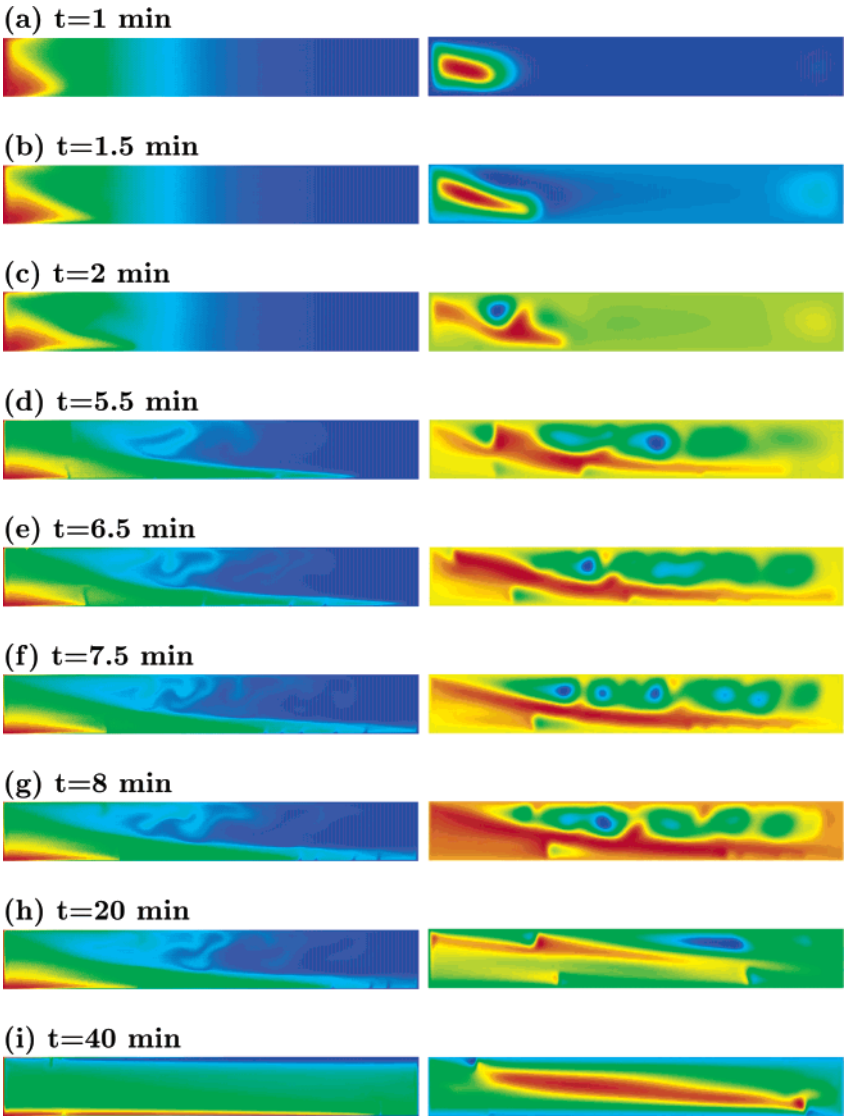

Figure 8. Monomer conversion (left) and stream lines (right) in the presence of convection (numerical simulation with $\beta_T \neq 0$, $\beta_C \neq 0$). Conversion and stream function data are as follows: (a) $t = 1$ min; conversion: blue = 0.000218, red = 0.0102; stream function: blue = 0, red = 0.00462; (b) $t = 1.5$ min; conversion: blue = 0.000326, red = 0.0153; stream function: blue = −0.000799, red = 0.00468; (c) $t = 2$ min; conversion: blue = 0.000435, red = 0.0204; stream function: blue = −0.0108, red = 0.00505; (d) $t = 5.5$ min; conversion: blue = 0.0012, red = 0.0557; stream function: blue = −0.0132, red = 0.00521l; (e) $t = 6.5$ min; conversion: blue = 0.00141, red = 0.0657; stream function: blue = −0.0136, red = 0.00486; (f) $t = 7.5$ min; conversion: blue = 0.00163, red = 0.0756; stream function: blue = −0.0139, red = 0.00482; (g) $t = 8$ min; conversion: blue = 0.00174, red = 0.0805; stream function: blue = −0.0185, red = 0.00363; (h) $t = 20$ min; conversion: blue = 0.00185, red = 0.0854; stream function: blue = −0.0145, red = 0.00436; (i) $t = 40$ min; conversion: blue = 0.00196, red = 0.0905; stream function: blue = −0.0138, red = 0.00481.

the reaction rate, which is given by

$$k(T) = s_2\sqrt{\frac{A_p^2}{A_t}}\exp\left(\frac{E_t - E_p}{RT}\right)$$

A_p and A_t are the pre-exponential factors for the propagation and termination steps, respectively, E_p and E_t are the respective activation energies for the propagation and termination steps, and R is the ideal gas constant.

The initiator consumption is dependent on the light intensity, which is given by the Burger-Lambert-Beer law:

$$J(d) = J_0 \exp[\epsilon(-d)]$$

where ϵ is a parameter that represents the product of the molar absorption coefficient multiplied by the initial initiator concentration, d is the distance from the enlightened boundary, and J_0 is the intensity of light projected on the illuminated side of the reactor.

In the Navier−Stokes equations (eqs 4 and 5), $\vec{U} = (u,v)$ is the two-dimensional velocity of the fluid, p is the pressure, ν is the kinematic viscosity, β_T is the thermal expansion coefficient, β_C shows the density dependence on the depth of conversion, T_0 is the initial temperature, g is the gravity acceleration, and $\vec{\gamma}$ is the unit vector in the vertical direction. We assume that the viscosity is constant.

The system of eqs 1−5 is considered in the rectangular domain $0 \leq x \leq L_x$ and $0 \leq y \leq L_y$, which represents a side view of the three-dimensional reactor. We use the no-flux boundary condition for the temperature and the free-surface boundary condition for the velocity. We do not need boundary conditions for C and I. The initial conditions are $\vec{U} = 0$, $T = T_0$, and $C = 0$ everywhere in the reactor.

3.2. Results. The stream function−vorticity formulation of the Navier−Stokes equations is used for the numerical simulations:

$$\frac{\partial \omega}{\partial t} + u\frac{\partial \omega}{\partial x} + v\frac{\partial \omega}{\partial y} - \nu\Delta\omega = \left(\beta_T\frac{\partial T}{\partial x} + \beta_C\frac{\partial C}{\partial x}\right)g \qquad (6)$$

$$-\Delta\Psi = \omega \qquad (7)$$

Here, Ψ is the stream function and ω is the vorticity:

$$u = \frac{\partial \Psi}{\partial y}$$

$$v = -\frac{\partial \Psi}{\partial x}$$

The free-surface boundary condition for the velocity can be written in terms of stream function−vorticity as follows:

$$\omega = 0$$

$$\Psi = 0$$

We use a finite-difference approximation and an alternating-directions method to solve the problem.

In the absence of convection ($\beta_T = \beta_C = 0$), the problem is reduced to three reaction−diffusion equations, corresponding to the temperature, the depth of conversion, and the initiator concentration. The front coordinate, as a function of time (Figure 2, curve 5), fits with the experimental data (Figure 2, curve 3). Gradients of the temperature, conversion, and initiator are formed in the direction of light illumination; the isolines are oriented vertical and parallel to each other. The depth of conversion in consecutive moments of time is shown in Figure 6.

If we consider the density dependence on the temperature but assume that it is independent of the depth of conversion ($\beta_T \neq 0$, $\beta_C = 0$), then convection essentially changes the front propagation. The exothermic chemical reaction begins near the left wall of the reactor. It heats the neighboring liquid, and then the preheated monomer rises to the top of the reactor and initiates the reaction there (see Figure 7b and c). Thus, we come to the paradoxal situation: the reaction is initiated from the left, but the front propagates from the top. Moreover, after some time, a second front is initiated at the illuminated (left) wall of the reactor but the front propagates from the top to the bottom.

We note that the same colors in Figure 7b−d can correspond to different values of the depth of conversion. Otherwise, it would be impossible to distinguish the details of the conversion distribution, because its variation inside the reactor for a given time can be rather weak. The same is done for the stream function. To determine the relationship between the colors and the values of conversion, we give the scale of colors (Figure 7a), and the values of conversion corresponding to blue and red. For example, in Figure 7b, for blue, the conversion equals 0.000218, whereas for red, it equals 0.0102. For all intermediate colors, the value of conversion can be obtained by linear interpolation. The similar approach is used in Figure 8.

The situation is quite different if the density is dependent both on the temperature and on the depth of conversion ($\beta_T \neq 0$, $\beta_C \neq 0$). At the beginning of the numerical simulations (see Figure 8a−c), the isolines of the conversion remain parallel to the illuminated side of the reactor, and then the down-flow motion that is also observed in the experiments (see Figure 4e) takes place, because the density of the polymer is greater than that of the monomer. Several minutes later, the upward motion of the preheated unreacted monomer initiates the reaction at the top of the reactor. After some time, the temperature and concentration distributions become practically uniform in space, and the reaction occurs throughout the entire volume of the reactor (see Figure 8d−h). This scenario is in good agreement with the experimental results.

4. Conclusions

The influence of weak convection (with rates of the order of 0.5 mm/s) on the photoinitiated polymerization is actually masked: the frontal character is retained, and the layers of polymerizing monomer carried out of the reaction region are so thin that they can be detected only by interferometric methods. However, convection essentially increases the rate of reaction propagation, which is no longer defined by the light intensity but by the monomer flow rate.

The polymerizing monomer that is washed out by the flow is capable of creating secondary polymerization fronts, which essentially contribute to generation of the final structure inhomogeneities.

As the convection intensity increases (to >1 mm/s), the frontal reaction character changes to volumetric. Therefore, the polymerization time decreases drastically, and we can observe the phenomenon of convective gel effect, i.e., spontaneous self-acceleration of the reaction and simultaneous polymerization of the entire monomer in the reactor due to convection.

Acknowledgment. This work is supported by the CNRS−RFBR program (under Grant No. PICS 1170/RFBR 01-01-22005 CNNI-a).

Nomenclature

A: pre-exponential factor
C: rate of conversion
E: activation energy
g: gravitational acceleration
I: initiator concentration
L: domain length
p: pressure
q: adiabatic heat release
R: gas constant
s_1, s_2: scaling coefficients
t: time
T: temperature
u, v: velocity components in the x- and y-direction, respectively
x, y: Cartesian coordinates

Greek Symbols

α: molar absorption coefficient
β_C: monomer expansion coefficient
β_T: thermal expansion coefficient
ϵ: absorption coefficient
κ: thermal diffusivity
ν: kinematic viscosity
Ψ: dimensionless stream function
ω: dimensionless vorticity

Subscripts

0: at initial time
x, y: in the x- or y-direction, respectively
p: propagation step
t: termination step

References and Notes

(1) Chechilo, N. M.; Enikolopyan, N. S. *Dokl. Phys. Chem. (Transl. of Dokl. Akad. Nauk)* **1974**, *214*, 174−176.

(2) Davtyan, S. P.; Zhirkov, P. V.; Volfson, S. A. *Russ. Chem. Rev.* **1984**, *53*, 150−163.

(3) Pojman, J. A.; Ilyashenko, V. M.; Khan, A. M. *J. Chem. Soc., Faraday Trans.* **1996**, *92*, 2825−2837.

(4) Pojman, J.; Volpert, Vit.; Volpert, Vl. *Self-Propagating High-Temperature Synthesis of Materials*; Borissov, A. A., De Luca, L. T., Merzhanov, A. G., Eds.; Taylor and Francis: New York, 2002; pp 98−118.

(5) Golubev, V. B.; Gromov, D. G.; Guseva, L. R.; Korolev, B. A.; Kostarev, K. G.; Lyubimova, T. P. *Heat Transfer Research* **1993**, *25*, (7), 888−893.

(6) Briskman, V. A.; Kostarev, K. G.; Lyubimova, T. P.; Levtov, V. L.; Mashinsky, A. L.; Nechitailo, G. S.; Romanov, V. V. *Acta Astronaut.* **1996**, *39*, (5), 395−402.

(7) McCaughey, B.; Pojman, J. A.; Simmons, C.; Volpert, V. A. *Chaos* **1998**, *8*, (2), 520−529.

(8) Garbey, M.; Taik, A.; Volpert, V. *Q. Appl. Math.* **1998**, *53*, 1−35.

(9) Bowden, G.; Garbey, M.; Ilyashenko, V. M.; Pojman, J. A.; Solovyov, S. E.; Taik, A.; Volpert, V. A. *J. Phys. Chem. B* **1997**, *101*, 678−686.

(10) Garbey, M.; Taik, A.; Volpert, V. *Q. Appl. Math.* **1996**, *54*, 225−247.

(11) Malkin, A. Ya.; Begishev, V. P.; Guseva, L. R.; Kostarev, K. G. *Polym. Sci., Ser. A (Transl. of Vysokomol. Soedin., Ser. A)* **1994**, *36*, 625−630.

(12) Kostarev, K. G.; Yudina, T. M.; Lysenko, S. N. *Polym. Sci., Ser. B (Transl. of Vysokomol. Soedin., Ser. B)* **1998**, *40*, (11−12), 386−390.

(13) Briskman, V. A.; Kostarev, K. G. *Proceedings of the International Aerospace Congress IAC-94*, August 15−19, 1994; The Scientific-Technical Company 'Petrovka' (STC 'Petrovka'): Moscow, Russia, 1995; Vol. 1, pp 514−525.

(14) Briskman, V. A.; Kostarev, K. G.; Lyubimova, T. P.; Levtov, V. L.; Romanov, V. V. *Cosmic Res. (Transl. of Kosm. Issled.)* **2001**, *39*, (4), 338−350.

(15) Kostarev, K. G.; Moshev, V. V.; Briskman, V. A. *Int. Polym. Sci. Technol.* **1998**, *25*, (4), 62−66.